Article

Modeling the Reaction Mechanisms of the Amide Hydrolysis in an *N*-(*o*-Carboxybenzoyl)-l-amino Acid

Zhijian Wu, Fuqiang Ban, and Russell J. Boyd

J. Am. Chem. Soc., **2003**, 125 (23), 6994-7000• DOI: 10.1021/ja021329i • Publication Date (Web): 17 May 2003

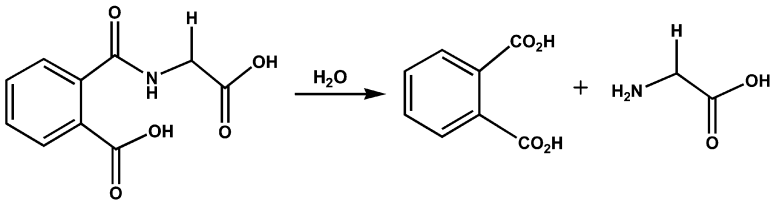

More About This Article

Additional resources and features associated with this article are available within the HTML version:

- Supporting Information
- Links to the 3 articles that cite this article, as of the time of this article download
- Access to high resolution figures
- Links to articles and content related to this article
- Copyright permission to reproduce figures and/or text from this article

View the Full Text HTML

J|A|C|S
ARTICLES
Published on Web 05/17/2003

Modeling the Reaction Mechanisms of the Amide Hydrolysis in an *N*-(*o*-Carboxybenzoyl)-L-amino Acid

Zhijian Wu, Fuqiang Ban, and Russell J. Boyd*

Contribution from the Department of Chemistry, Dalhousie University, Halifax, Nova Scotia, B3H 4J3, Canada

Received November 4, 2002; E-mail: russell.boyd@dal.ca

Abstract: Reaction mechanisms of the amide hydrolysis from the protonated, neutral, and deprotonated forms of *N*-(*o*-carboxybenzoyl)-L-amino acid have been investigated by use of the B3LYP density functional method. Our calculations reveal that in the amide hydrolysis the reaction barrier is significantly lower in solution than that in the gas phase, in contrast with the mechanism for imide formation in which the solvent has little influence on the reaction barrier. In the model reactions, the water molecules function both as a catalyst and as a reactant. The reaction mechanism starting from the neutral form of *N*-(*o*-carboxybenzoyl)-L-amino acid, which corresponds to pH 0−3, is concluded to be the most favored, and a concerted mechanism is more favorable than a stepwise mechanism. This conclusion is in agreement with experimental observations that the optimal pH range for amide hydrolysis of *N*-(*o*-carboxybenzoyl)-L-leucine is pH 0−3 where *N*-(*o*-carboxybenzoyl)-L-leucine is predominantly in its neutral form. We suggest that besides the acid-catalyzed mechanism the addition−elimination mechanism is likely to be an alternative choice for cleaving an amide bond. For the reaction mechanism initiated by protonation at the amidic oxygen (hydrogen ion concentration $H_0 < -1$), the reaction of the model compound with two water molecules lowers the transition barrier significantly compared with that involving a single water molecule.

1. Introduction

Intramolecular catalysis has received much attention as the basic model for enzyme catalysis and remains an active field.[1−5] A crucial element of intramolecular models for enzyme catalysis is the way in which the reacting catalytic and substrate groups are held close together on the same molecule. The important advantage over intermolecular catalysis is that the structure of a system performing intramolecular catalysis, and in particular the geometry of the interaction between functional groups, can be fully defined. Studies on enzyme reaction mechanisms, including intramolecular catalysis, are ideal for interdisciplinary collaborations among biochemists, organic chemists, and physical chemists. The purpose of studying intramolecular systems is to mimic and understand the various reaction mechanisms by use of simple models that can provide insight into more complicated enzyme catalytic mechanisms.

As models for hydrolytic enzymes, there has been considerable interest in the chemistry of intramolecular catalysis of amide hydrolysis by the neighboring carboxyl group both theoretically[6−14] and experimentally.[15−26] Among experimental studies, the recently synthesized molecules containing two carboxyl groups,[24,25] *N*-(*o*-carboxybenzoyl)-L-phenylalanine, *N*-(*o*-carboxybenzoyl)-L-leucine, and *N*-(*o*-carboxybenzoyl)-L-valine, are especially interesting because they provide potential models for the study of the catalytic mechanisms of aspartic proteinases.[27] As shown experimentally,[15−26] cyclization to the imide and amide hydrolysis are the two main types of reactions. Imide formation predominates under highly acidic conditions

(1) Rabenstein, D. L.; Shi, T.; Spain, S. *J. Am. Chem. Soc.* **2000**, *122*, 2401.
(2) Cox, C.; Lectka, T. *J. Am. Chem. Soc.* **1998**, *120*, 10660.
(3) Hartwell, E.; Hodgson, D. R. W.; Kirby, A. J. *J. Am. Chem. Soc.* **2000**, *122*, 9326.
(4) Bowden, K.; Brownhill, A. *J. Chem. Soc., Perkin Trans. 2* **1997**, 219.
(5) Barber, S. E.; Dean, K. E. S.; Kirby, A. J. *Can. J. Chem*. **1999**, *77*, 792.
(6) Yunes, S. F.; Gesser, J. Chaimovich, C. H.; Nome, F. *J. Phys. Org. Chem.* **1997**, *10*, 461.
(7) Barros, T. C.; Yunes, S.; Menegon, G.; Nome, F.; Chaimovich, H.; Politi, M. J.; Dias, L. G.; Cuccovia, I. M. *J. Chem. Soc., Perkin Trans. 2* **2001**, 2342.
(8) Park, H.; Suh, J.; Lee, S. *THEOCHEM* **1999**, *490*, 47.
(9) Hori, K.; Kamimura, A.; Ando, K.; Mizumura, M.; Ihara, Y. *Tetrahedron* **1997**, *53*, 4317.
(10) Antonczak, S.; Ruiz-López, M. F.; Rivail, J. L. *J. Am. Chem. Soc.* **1994**, *116*, 3912.
(11) Antonczak, S.; Ruiz-López, M. F.; Rivail, J. L. *J. Mol. Model.* **1997**, *3*, 434.
(12) Bakowies, D.; Kollman, P. A. *J. Am. Chem. Soc.* **1999**, *121*, 5712.
(13) Guo, J.-X.; Ho, J.-J. *J. Phys. Chem. A* **1999**, *103*, 6433.
(14) Naundorf, H.; Worth, G. A.; Meyer, H.-D.; Kühn, O. *J. Phys. Chem. A* **2002**, *106*, 719.
(15) Perry, C. J. *J. Chem. Soc., Perkin Trans. 2* **1997**, 977.
(16) Granados, A. M.; de Rossi, R. H. *J. Org. Chem.* **2001**, *66*, 1548.
(17) Bender, M. L.; Chow, Y.-L.; Chloupek, F. *J. Am. Chem. Soc.* **1958**, *80*, 5380.
(18) Brown, J.; Su, S. C.; Shafer, J. A. *J. Am. Chem. Soc.* **1966**, *88*, 4468.
(19) Hawkins, M. D. *J. Chem. Soc., Perkin Trans. 2* **1976**, 642.
(20) Aldersley, M. F.; Kirby, A. J.; Lancaster, P. W. *J. Chem. Soc., Perkin Trans. 2* **1974**, 1504.
(21) Aldersley, M. F.; Kirby, A. J.; Lancaster, P. W.; McDonald, R. S.; Smith, C. R. *J. Chem. Soc., Perkin Trans. 2* **1974**, 1487.
(22) Kirby, A. J.; McDonald, R. S.; Smith, C. R. *J. Chem. Soc., Perkin Trans. 2* **1974**, 1495.
(23) Kirby, A. J.; Lancaster, P. W. *J. Chem. Soc., Perkin Trans. 2* **1972**, 1206.
(24) Onofrio, A. B.; Joussef, A. C.; Nome, F. *Synth. Commun.* **1999**, *29*, 3039.
(25) Onofrio, A. B.; Gesser, J. C.; Joussef, A. C.; Nome, F. *J. Chem. Soc., Perkin Trans. 2* **2001**, 1863.
(26) Fife, T. H.; Chauffe, L. *J. Org. Chem*. **2000**, *65*, 3579.
(27) Meek, T. D. Catalytic mechanisms of the aspartic proteinases. In *Comprehensive Biological Catalysis: A Mechanistic Reference*; Sinott, M., Ed.; Academic Press: San Diego, CA, 1998; Chapter 8.

10.1021/ja021329i CCC: $25.00

Scheme 1. Hydrolysis Reaction of the Model System of *N*-(*o*-Carboxybenzoyl)glycine

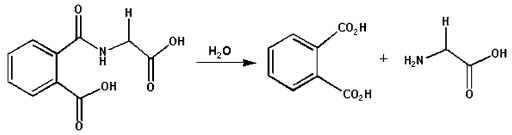

($H_0 < -1$), while amide hydrolysis is observed in the $H_0 > -1$ to pH 5. Possible reaction mechanisms have been proposed on the basis of experimental studies.[25]

In our previous paper,[28] we reported the results of a computational study of the imide formation of the model compound *N*-(*o*-carboxybenzoyl)-L-amino acid. The results indicated that the reaction initiated by protonation at the oxygen of the carboxyl group of the amino acid is favored, while those initiated by deprotonation at the oxygen of the carboxyl group of phthalic acid and at the amidic nitrogen are minor pathways. These conclusions are in good agreement with the experimental observations.[25] In this paper, we report the amide hydrolysis of our model compound *N*-(*o*-carboxybenzoyl)glycine (see Scheme 1) using the same method. Possible mechanisms of amide hydrolysis proposed on the basis of experimental evidence[25] are summarized in Scheme 2. In the range of hydrogen ion concentration $H_0 < -1$, the proposed mechanism is **1** → **2** → **3** → **4** → **5**, in which the intermediates are cationic. At pH 0−3, the routes are either **1** → **6** → **7** (concerted mechanism) or **1** → **8** → **6** → **7** and **1** → **8** → **9** → **6** → **7** (stepwise mechanisms). The intermediates are neutral or zwitterionic except for the cationic species **9**. At pH 3−5, the route is **1** → **10** → **11** → **12** → **13**, in which the intermediates are anionic. To obtain further insight into the reaction mechanism and reduce the computational cost, a theoretical study on the model compound *N*-(*o*-carboxybenzoyl)glycine has been carried out using density functional theory.

2. Computational Methods

All geometry optimizations were performed with the B3LYP hybrid density functional in conjunction with the 6-31G(d,p) basis set using the Gaussian 98 suite of programs.[29] The B3LYP functional is a combination of Becke's three-parameter hybrid exchange functional,[30,31] as implemented in Gaussian 98,[32] and the Lee−Yang−Parr correlation functional.[33] Harmonic vibrational frequencies and zero-point vibrational energies (ZPVEs) were obtained at the same level of theory. Relative energies were obtained by performing single-point calculations at the B3LYP level with the 6-311G(2df,p) basis set using the above optimized geometries and by including the zero-point vibrational energy, i.e., B3LYP/6-311G(2df,p)//B3LYP/6-31G(d,p) + ZPVE. The entropy contributions to the free energies at 298.15 K were derived from B3LYP/6-31G(d,p) frequency calculations.

The Onsager[34] and the conductor-like polarized continuum (CPCM)[35] solvent models of the self-consistent reaction field approach have been employed to investigate the solvent effect by treating the solvent as a polarizable continuum with a dielectric constant and embedding the solute molecule in a cavity of the dielectric continuum. The cavity defined by the Onsager model is a fixed spherical sphere in the simplest approximation, while the CPCM method defines a more realistic cavity enabling a more accurate description of the solvent effects. Relative to the Onsager model, the CPCM model provides more reliable energies[35,37−41] in solution.

Ideally, the geometry optimizations and frequency calculations and single-point energy calculations should have been done using the CPCM model. However, we encountered convergence problems in optimizing several structures of this study, as also noted in the work of Vallet et al.[40] To overcome this problem, we obtained all the structures in solution by using the Onsager method, which has been shown to be very reliable and effective for geometry optimizations and frequency calculations.[36] Thus, the solvent effect on the potential energy surface was investigated by a hybrid approach of single-point calculations at the B3LYP/6-311G(2df,p) level using the CPCM model (denoted CPCM-B3LYP/6-311G(2df,p)) on the geometries obtained by using the Onsager model with a dielectric constant of 78.39 at the B3LYP/6-31G(d,p) level (denoted Onsager-B3LYP/6-31G(d,p)). The zero-point energy corrections obtained from the Onsager-B3LYP/6-31G(d,p) frequency calculations are included in the calculations of the relative energies in the solvation of water, i.e., CPCM-B3LYP/6-311G(2df,p)//Onsager-B3LYP/6-31G(d,p) + ZPVE. The entropy contributions to the free energies in solution at 298.15 K were derived from Onsager-B3LYP/6-31G(d,p) frequency calculations. All energies are in kJ mol^{-1}.

3. Results and Discussion

The computed energy profiles are shown in Figures 1−10. Figures 1−5 include only the ZPVE correction, while the entropy contribution at 298.15 K is also included in Figures 6−10.

3.1. Reaction Mechanism 1 → 2 → 3 → 4 → 5 of Protonated *N*-(*o*-Carboxybenzoyl)-L-amino Acid (Hydrogen Ion Concentration $H_0 < -1$). In this route, two mechanisms are studied. One is the reaction of the model compound with a single water molecule, and the other is with two water molecules. Of course, a looser transition state with more than two water molecules may also be possible, but such a transition state is difficult to locate at the present level of theory. Therefore, in this paper we focus on the cases with one and two water molecules only. We will use "**a**" to represent the conformers in the case of a single water molecule and "**b**" to represent those in the presence of two water molecules. In both cases, the initial reactant **1** has the same geometry. The protonation of **1** gives **2** (Scheme 2). The proton affinity of **1** at the amidic oxygen is 940.9 kJ mol^{-1}, indicating that the initial reactant **1** can be protonated easily.

(28) Wu, Z.; Ban, F.; Boyd, R. J. *J. Am. Chem. Soc.* **2003**, *125*, 3642.
(29) Frisch, M. J.; Trucks, G. W.; Schlegel, H. B.; Scuseria, G. E.; Robb, M. A.; Cheeseman, J. R.; Zakrzewski, V. G.; Montgomery, J. A., Jr.; Stratmann, R. E.; Burant, J. C.; Dapprich, S.; Millam, J. M.; Daniels, A. D.; Kudin, K. N.; Strain, M. C.; Farkas, O.; Tomasi, J.; Barone, V.; Cossi, M.; Cammi, R.; Mennucci, B.; Pomelli, C.; Adamo, C.; Clifford, S.; Ochterski, J.; Petersson, G. A.; Ayala, P. Y.; Cui, Q.; Morokuma, K.; Malick, D. K.; Rabuck, A. D.; Raghavachari, K.; Foresman, J. B.; Cioslowski, J.; Ortiz, J. V.; Stefanov, B. B.; Liu, G.; Liashenko, A.; Piskorz, P.; Komaromi, I.; Gomperts, R.; Martin, R. L.; Fox, D. J.; Keith, T.; Al-Laham, M. A.; Peng, C. Y.; Nanayakkara, A.; Gonzalez, C.; Challacombe, M.; Gill, P. M. W.; Johnson, B. G.; Chen, W.; Wong, M. W.; Andres, J. L.; Head-Gordon, M.; Replogle, E. S.; Pople, J. A. *Gaussian 98*, Rev A.7; Gaussian, Inc.: Pittsburgh, PA, 1998.
(30) Becke, A. D. *J. Chem. Phys.* **1993**, *98*, 1372.
(31) Becke, A. D. *J. Chem. Phys.* **1993**, *98*, 5648.
(32) Stephens, P. J.; Devlin, F. J.; Chabalowski, C. F.; Frisch, M. J. *J. Phys. Chem.* **1994**, *98*, 11623.
(33) Lee, C.; Yang, W.; Parr, R. G. *Phys. Rev. B* **1988**, *37*, 785.
(34) Onsager, L. *J. Am. Chem. Soc.* **1936**, *58*, 1486.
(35) Barone, V.; Cossi, M. *J. Phys. Chem. A* **1998**, *102*, 1995.
(36) (a) Wong, M. W.; Frisch, M. J.; Wiberg, K. B. *J. Am. Chem. Soc.* **1991**, *113*, 4776. (b) Wong, M. W.; Wiberg, K. B.; Frisch, M. J. *J. Am. Chem. Soc.* **1992**, *114*, 523. (c) Wong, M. W.; Wiberg, K. B.; Frisch, M. J. *J. Am. Chem. Soc.* **1992**, *114*, 1645. (d) Wong, M. W.; Wiberg, K. B.; Frisch, M. J. *J. Chem. Phys.* **1991**, *95*, 8991.
(37) Liptak, M. D.; Shields, G. C. *J. Am. Chem. Soc.* **2001**, *123*, 7314.
(38) Hölscher, M.; Keul, H.; Höcher, H. *Macromolecules* **2002**, *35*, 8194.
(39) Nonnenberg, C.; van der Donk, W. A.; Zipse, H. *J. Phys. Chem. A* **2002**, *106*, 8708.
(40) Vallet, V.; Wahlgren, U.; Schimmelpfennig, B.; Szabó, Z.; Grenthe, I. *J. Am. Chem. Soc.* **2001**, *123*, 11999.
(41) Bahmanyar, S.; Houk, K. N. *J. Am. Chem. Soc.* **2001**, *123*, 11999.

Scheme 2. Summary of the Experimentally Proposed Schematic Routes for Amide Hydrolysis

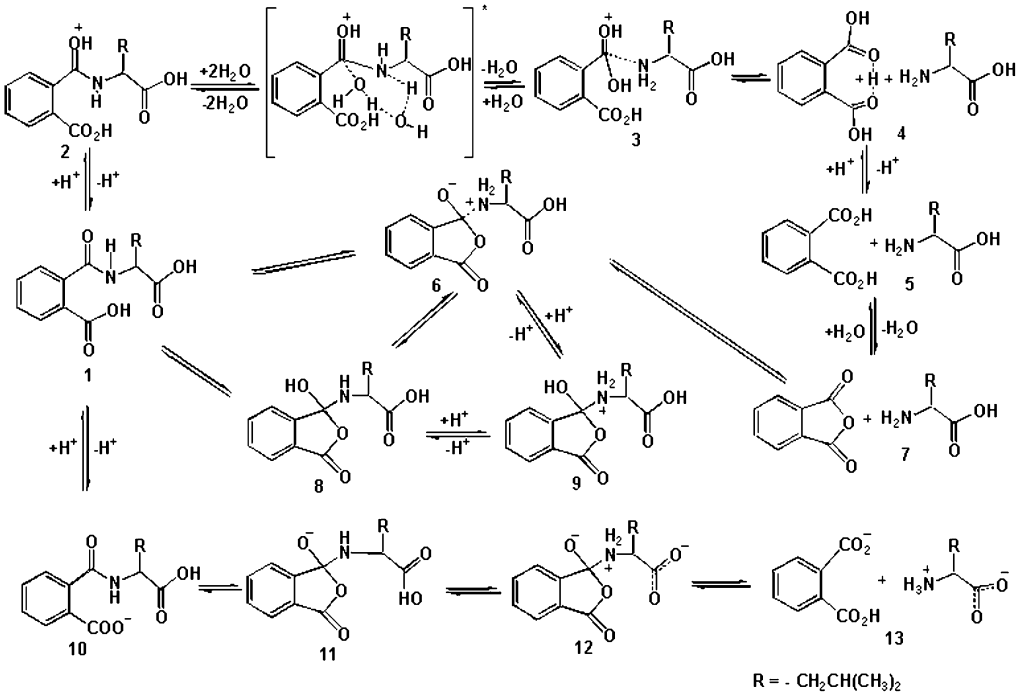

3.1.i. Hydrolytic Reaction with a Single Water Molecule. In the gas phase (Figure 1), complex **2a** lies lower than **2** + H_2O by 58.3 kJ mol^{-1}. **TSa** has an energy of 154.6 kJ mol^{-1} relative to **2** + H_2O. Product **3** and the separated system **4** have an energy of 21.8 and 33.8 kJ mol^{-1}, respectively, compared with **2** + H_2O. In solution, the solvent raises the energies of **2a**, **TSa**, and **3** by 49.8, 41.5, and 24.0 kJ mol^{-1}, respectively, but lowers **4** by 5.3 kJ mol^{-1}. Clearly, the water molecule participates in the reaction as a reactant.

3.1.ii. Water-Catalyzed Reaction with Two Water Molecules. To release the geometric tension of the four-membered ring transition state **TSa**, a second water may participate in the reaction as a catalyst. From Figure 2, one can see that in the gas phase **2b** lies lower than the separated system **2** + 2H_2O by 89.5 kJ mol^{-1}. The energy of **TSb** is 78.1 kJ mol^{-1} higher than **2** + 2H_2O. Product **3b** has a relative energy of −19.5 kJ mol^{-1}. The separated systems **3** + H_2O and **4** + H_2O lie higher than **2** + 2H_2O by 43.0 and 54.9 kJ mol^{-1}, respectively. On the other hand, in solution, the solvent has a significant influence on the reaction. It increases the energies of **2b**, **TSb**, **3b**, and complex **3** + H_2O by 81.0, 48.2, 63.0, and 14.1 kJ mol^{-1}, respectively, but lowers complex **4** + H_2O by 15.1 kJ mol^{-1}.

Figures 1 and 2 indicate that the energy barrier **TSb** of the reaction involving two water molecules is much lower than that

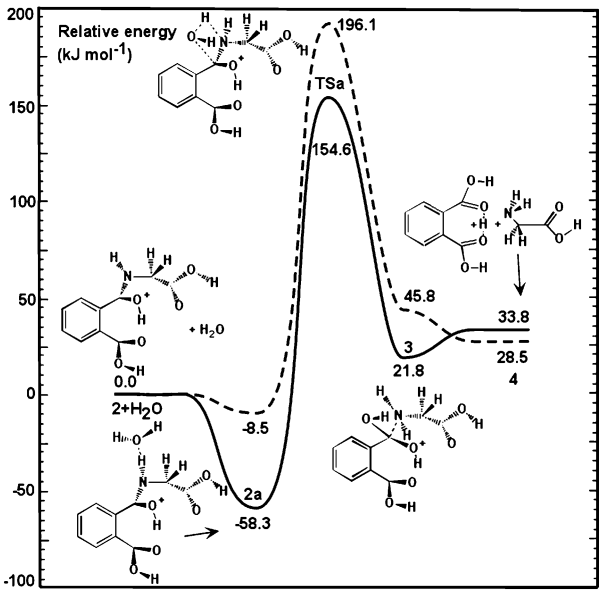

Figure 1. Schematic energy profile at 0 K for the route **2** + H_2O → **2a** → **3** → **4** with a single water molecule involved in the amide hydrolysis. The solid line represents the gas phase, and the dashed line represents the solution.

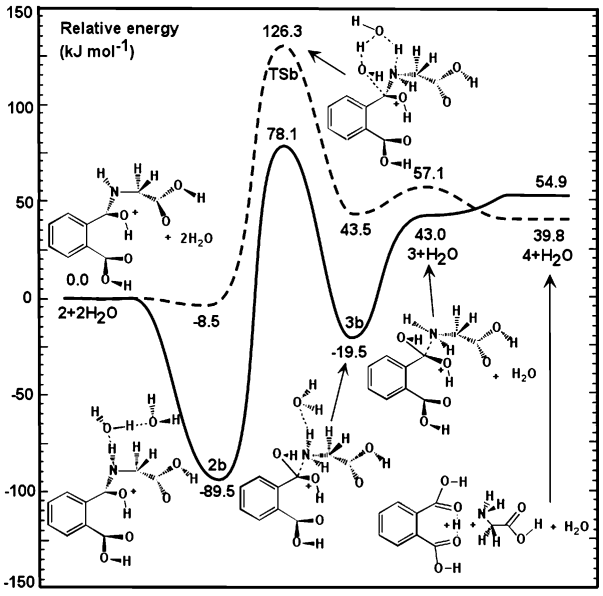

Figure 2. Schematic energy profile at 0 K for the route **2** + 2H_2O → **2b** → **3b** → **3** + H_2O → **4** + H_2O with two water molecules involved in the amide hydrolysis. The solid line represents the gas phase, and the dashed line represents the solution.

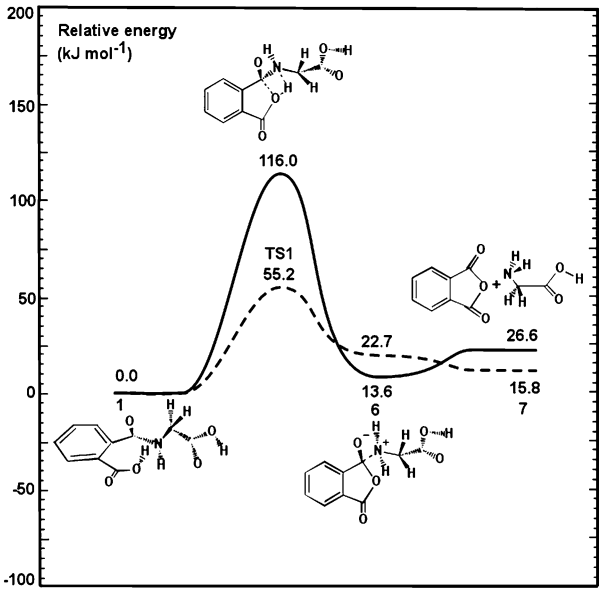

Figure 3. Schematic energy profile at 0 K for the concerted mechanism **1** → **6** → **7**. The solid line represents the gas phase, and the dashed line represents the solution.

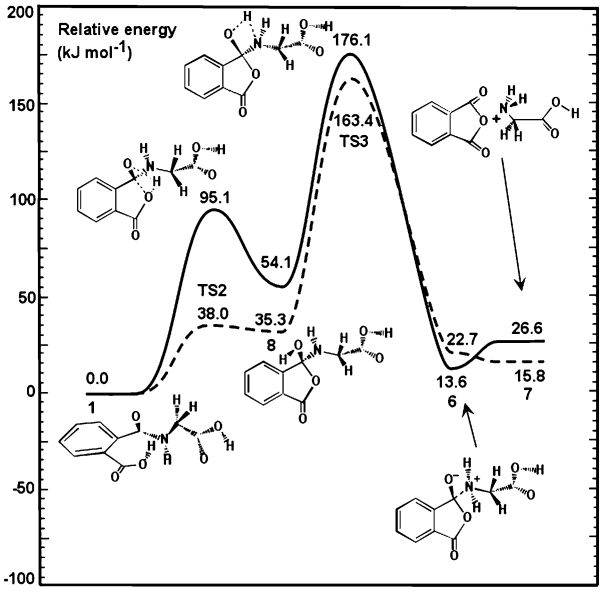

Figure 4. Schematic energy profile at 0 K for the stepwise direct proton-transfer mechanism **1** → **8** → **6** → **7**. The solid line represents the gas phase, and the dashed line represents the solution.

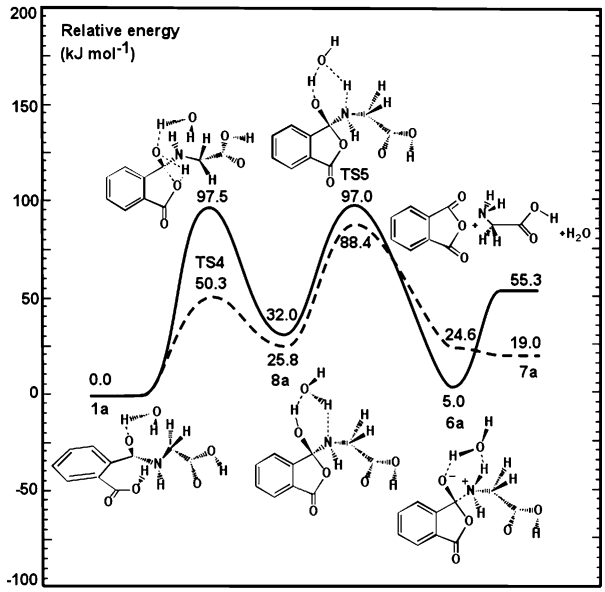

Figure 5. Schematic energy profile at 0 K for the stepwise water-catalyzed proton-transfer mechanism **1a** → **8a** → **6a** → **7a**. The solid line represents the gas phase, and the dashed line represents the solution.

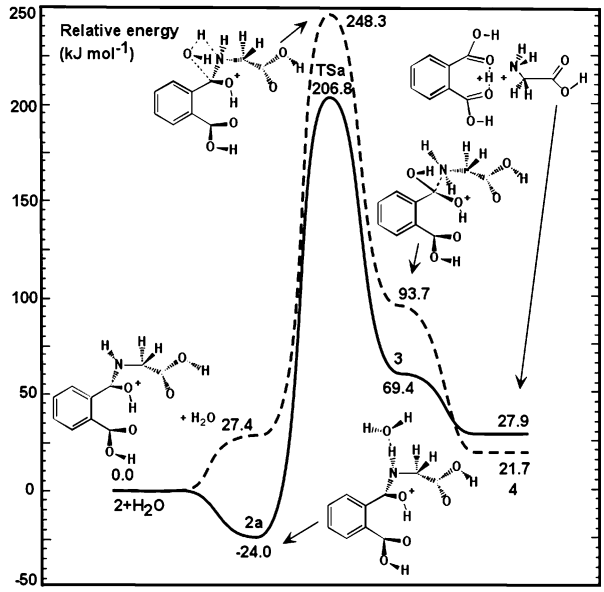

Figure 6. Schematic energy profile at 298.15 K for the route **2** + H_2O → **2a** → **3** → **4** with a single water molecule involved in the amide hydrolysis. The solid line represents the gas phase, and the dashed line represents the solution.

involving a single water molecule (**TSa**) for both the gas phase and solution. For the former, the barriers from **2b** are 167.6 kJ mol^{-1} in the gas phase and 134.8 kJ mol^{-1} in solution, while for the latter the barriers from **2a** are 212.9 kJ mol^{-1} in the gas phase and 204.6 kJ mol^{-1} in solution. This means that the reaction involving two water molecules lowers the barrier significantly and makes the reaction proceed easily. Water functions not only as a solvent but also as a reactant and as a catalyst.

The entropy-corrected energy profiles at 298.15 K show similar patterns for both a single water molecule (Figure 6) and two water molecules (Figure 7). For the latter case, the energy barrier **TSb** in the entropy-corrected case is 192.4 kJ mol^{-1} in solution (from **2** + $2H_2O$) and 188.0 kJ mol^{-1} (from **2b**) in the gas phase as shown in Figure 7. These barriers are higher than those in the ZPVE-only corrected case (134.8 kJ mol^{-1} in solution and 167.6 kJ mol^{-1} in the gas phase from **2b** as shown in Figure 2). The increase in energy barriers in the entropy-corrected case for both the gas phase and solution is also observed for **TSa** in the single water molecule case (Figures 1 and 6).

3.2. Reaction Mechanisms from Neutral *N*-(*o*-Carboxybenzoyl)-L-amino Acid (pH 0−3). There are several reaction mechanisms for the C−N bond cleavage at pH 0−3. The reaction may proceed through either a concerted mechanism **1** → **6** → **7** (by C−O bond formation and simultaneous proton transfer from the carboxyl group of the phthalic acid to the amidic nitrogen, leading to C−N bond cleavage; see Scheme 2) or stepwise mechanisms **1** → **8** → **6** → **7** (for which the first

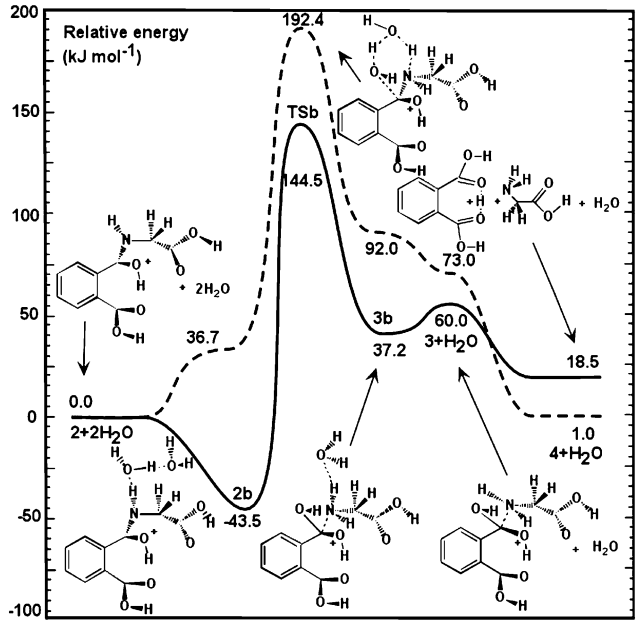

Figure 7. Schematic energy profile at 298.15 K for the route **2** + $2H_2O$ → **2b** → **3b** → **3** + H_2O → **4** + H_2O with two water molecules involved in the amide hydrolysis. The solid line represents the gas phase, and the dashed line represents the solution.

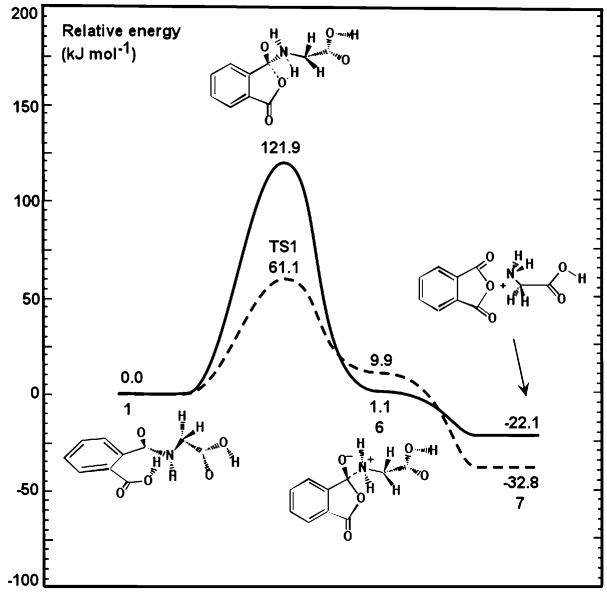

Figure 8. Schematic energy profile at 298.15 K for the concerted mechanism **1** → **6** → **7**. The solid line represents the gas phase, and the dashed line represents the solution.

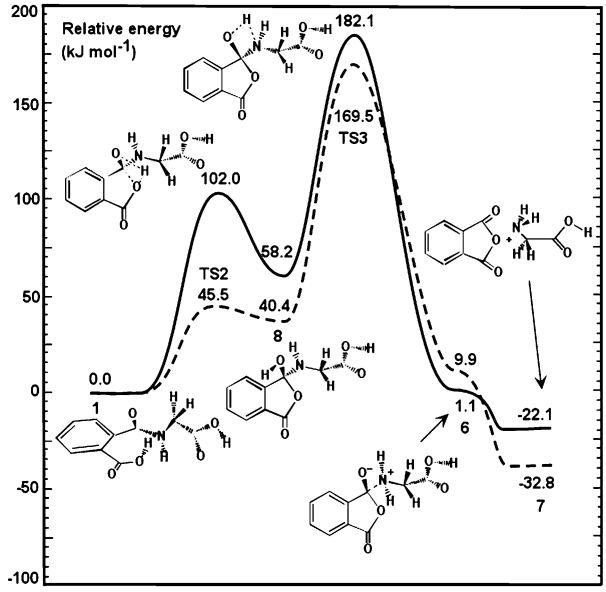

Figure 9. Schematic energy profile at 298.15 K for the stepwise direct proton-transfer mechanism **1** → **8** → **6** → **7**. The solid line represents the gas phase, and the dashed line represents the solution.

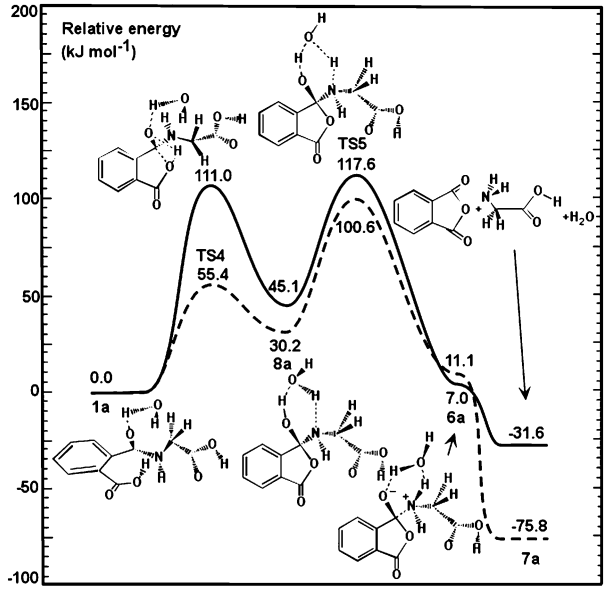

Figure 10. Schematic energy profile at 298.15 K for the stepwise water-catalyzed proton-transfer mechanism **1a** → **8a** → **6a** → **7a**. The solid line represents the gas phase, and the dashed line represents the solution.

step of the reaction is the C−O bond formation and simultaneous proton transfer from the carboxyl group of the phthalic acid to the amidic oxygen **1** → **8** followed by proton transfer from the amidic oxygen to the amidic nitrogen **8** → **6**) and **1** → **8** → **9** → **6** → **7** (for which the protonation of **8** on the amidic nitrogen to form **9** and the deprotonation of **9** at the amidic oxygen to form **6** proceed separately; i.e., no proton transfer occurs). In the stepwise mechanism **1** → **8** → **6** → **7**, the proton transfer from **8** to form **6** can be either direct (this corresponds to **1** → **8** → **6** → **7**, Figures 4 and 9) or through a water molecule (this corresponds to **1a** → **8a** → **6a** → **7a**, Figures 5 and 10). In fact, all the above-mentioned mechanisms are the addition−elimination mechanism that is equivalent to the overall outcome of the corresponding amide hydrolysis reaction.

In this part, **TS1** in Figure 3 denotes the transition state in the concerted mechanism **1** → **6** → **7**. In the stepwise mechanism **1** → **8** → **6** → **7**, **TS2** in Figure 4 denotes the transition state of C−O bond formation and simultaneous proton transfer from the carboxyl group of the phthalic acid to the amidic oxygen between **1** and **8**, and **TS3** in Figure 3 denotes the direct proton transfer between **8** and **6**. In the stepwise mechanism **1a** → **8a** → **6a** → **7a**, **TS4** in Figure 5 denotes the transition state between **1a** and **8a** that is formed by water hydrogen-bonded to the amidic oxygen of **TS2**, and **TS5** in Figure 5 denotes the proton transfer through a water molecule between **8a** and **6a**.

3.2.i. Concerted Mechanism 1 → 6 → 7. From Figure 3, one can see that the solvent significantly lowers the reaction

barrier. In the gas phase, it costs 116.0 kJ mol^{-1} to form **6** from **1**, while in solution, only 55.2 kJ mol^{-1} is required to make the reaction occur. This means that in solution the energy barrier **TS1** drops to one-half of that in the gas phase. For **6**, the energy in solution is 9.1 kJ mol^{-1} higher than in the gas phase, while for the separated system **7**, the solvent lowers the energy by 10.8 kJ mol^{-1}. In this part, it is clear that the C−N bond is cleaved by an elimination mechanism caused by the intramolecular C−O bond formation and a simultaneous proton transfer from the carboxyl group of phthalic acid to the amidic nitrogen.

The entropy-corrected energy profile at 298.15 K (Figure 8) shows the same pattern. The energy barrier **TS1** is about 6 kJ mol^{-1} higher than that in the ZPVE-only corrected case for both phases.

3.2.ii. Stepwise Mechanism 1 → 8 → 6 → 7 of Direct Proton Transfer. In the gas phase, the first barrier to overcome **TS2** is 95.1 kJ mol^{-1} (Figure 4). After the formation of the C−O bond and the simultaneous proton transfer from the carboxyl group of phthalic acid to the amidic oxygen, intermediate **8** is formed. **8** lies higher than the initial reactant **1** by 54.1 kJ mol^{-1}. For the direct proton transfer, the energy of **TS3** is 176.1 kJ mol^{-1} higher than that of **1**, and the reaction proceeds to give product **6** with a relative energy of 13.6 kJ mol^{-1}. The separated system **7** lies higher than **1** by 26.6 kJ mol^{-1}.

In solution, the first energy barrier **TS2** drops significantly (by 57.1 kJ mol^{-1}) compared with that in the gas phase. It only costs 38.0 kJ mol^{-1} to form intermediate **8**. For the subsequent direct proton transfer, the relative energy of **TS3** in solution is 12.7 kJ mol^{-1} lower than in the gas phase compared with **1**.

The entropy-corrected profile at 298.15 K shows a similar pattern (Figure 9). The energy barriers **TS2** and **TS3** are only slightly increased compared with those in the ZPVE-only corrected case (Figure 4). On the basis of our calculation, it is clear that the stepwise mechanism **1 → 8 → 6 → 7** is not competitive with the concerted mechanism **1 → 6 → 7** for both the gas phase and solution.

3.2.iii. Stepwise Mechanism 1a → 8a → 6a → 7a of Proton Transfer through a Water Molecule. In this mechanism, the proton transfer from **8** to form **6** occurs via a water molecule (Scheme 2); that is, the water molecule functions as a catalyst.

For the ZPVE-only corrected case (Figure 5), it can be seen that **TS4** is 97.5 kJ mol^{-1} higher than **1a** in the gas phase, while in solution it drops significantly, having a relative energy of 50.3 kJ mol^{-1} compared with **1a**. After the C−O bond formation and simultaneous proton transfer from the carboxyl group of the phthalic acid to the amidic oxygen, the intermediate **8a** is formed, which lies higher than the initial reactant **1a** by 32.0 kJ mol^{-1} in the gas phase and 25.8 kJ mol^{-1} in solution. For proton transfer through a water molecule, **TS5** has a relative energy of 97.0 kJ mol^{-1} in the gas phase, which is nearly the same as that of **TS4**, and 88.4 kJ mol^{-1} in solution, which is 38.1 kJ mol^{-1} higher than that of **TS4**. This indicates that the transition barrier **TS4** drops significantly because of solvent effects. The reaction proceeds to give product **6a**, which has an energy of 5.0 kJ mol^{-1} in the gas phase and 24.6 kJ mol^{-1} in solution compared with **1a**. The separated system **7a** lies higher than **1a** by 55.3 kJ mol^{-1} in the gas phase and 19.0 kJ mol^{-1} in solution.

For the entropy-corrected case at 298.15 K (Figure 10), **TS4**, **8a**, and **TS5** are raised a little compared with the ZPVE-only corrected case (Figure 5), while **6a** and **7a** drop. In particular, the separated system **7a** drops significantly, having an energy of −31.6 kJ mol^{-1} in the gas phase and −75.8 kJ mol^{-1} in solution compared with **1a**, while in the ZPVE-only corrected case **7a** is higher than the initial reactant **1a** for both phases (Figure 5).

From our previous results, it is known that to form **6** from **8** in the stepwise mechanism **1 → 8 → 6 → 7**, 122.0 kJ mol^{-1} (**TS3**) is required in the gas phase and 128.1 kJ mol^{-1} in solution (Figure 4), while it only costs 65.0 kJ mol^{-1} (**TS5**) in the gas phase and 62.6 kJ mol^{-1} in solution if proton transfer occurs through a water molecule (**8a → 6a** in Figure 5). On the other hand, compared with the initial reactant, **TS5** (97.0 kJ mol^{-1} in the gas phase and 88.4 kJ mol^{-1} in solution, Figure 5) is also much lower than **TS3** (176.1 kJ mol^{-1} in the gas phase and 163.4 kJ mol^{-1} in solution, Figure 4). This indicates that the transition barrier is significantly lowered if a water molecule participates in the proton-transfer reaction as a catalyst. Once again, water acts as both a solvent and a catalyst.

It is also interesting that in the gas phase the transition barriers of the concerted mechanism **1 → 6 → 7** for both the ZPVE-only corrected case (116.0 kJ mol^{-1} in Figure 3) and the entropy-corrected case at 298.15 K (121.9 kJ mol^{-1} in Figure 8) are competitive with the stepwise mechanism of proton transfer through a water molecule **1a → 8a → 6a → 7a** because **TS4** and **TS5** of the proton transfer through a water molecule is 97.5 and 97.0 kJ mol^{-1}, respectively, for the ZPVE-only corrected case (Figure 5) and 111.0 and 117.6 kJ mol^{-1}, respectively, for the entropy-corrected case at 298.15 K (Figure 10) compared with the initial reactant **1a**. However, in solution the concerted mechanism (with transition barrier 55.2 kJ mol^{-1} for the ZPVE-only corrected case in Figure 3 and 61.1 kJ mol^{-1} for the entropy-corrected case at 298.15 K in Figure 8) is preferred because **TS5** has an energy of 88.4 kJ mol^{-1} for the ZPVE-only corrected case (Figure 5) and 100.6 kJ mol^{-1} for the entropy-corrected case at 298.15 K (Figure 10) compared with **1a** (although **TS4** is competitive with **TS1**). This indicates that solvent effects play an important role in biological systems, as in the model systems of this study, and that conclusions based on only gas-phase calculations may be misleading. Therefore, our conclusion is that, compared with the concerted mechanism **1 → 6 → 7**, the stepwise pathways including proton transfer through a water molecule are still less favorable.

It is apparent that for the transition states of the proton transfer, **TS3** and **TS5** (either directly or through a water molecule), the solvent has little influence on the energy barriers. The barrier in solution is only slightly lower than in the gas phase.

3.2.iv. Stepwise Mechanism 1 → 8 → 9 → 6 → 7. For this route, the first step **1 → 8** is identical to the results shown in Figures 4 and 9. Then (see Scheme 2) **8** can be protonated at the amidic nitrogen to form **9** with a proton affinity of 908.2 kJ mol^{-1}. It costs 851.0 kJ mol^{-1} to deprotonate at the amidic oxygen of **9** to form **6**. This mechanism is also possible in biological processes.

In brief, the concerted mechanism is more favorable than the stepwise mechanisms for pH 0−3. This conclusion is in agreement with experimental observations[25] that the optimal pH

for amide hydrolysis of *N*-(*o*-carboxybenzoyl)-L-leucine lies between 0 and 3 where *N*-(*o*-carboxybenzoyl)-L-leucine is predominantly in its neutral form. Compared with direct proton transfer, the transition barrier will be significantly lowered if a water molecule participates in the proton-transfer reaction as a catalyst.

3.3. Reaction Mechanism 1 → 10 → 11 → 12 → 13 of Deprotonated *N*-(*o*-Carboxybenzoyl)-L-amino Acid (pH 3−5). For the first step of the reaction, structure **11** (Scheme 2) was not obtained in our calculations because no C−O bond was formed. Therefore, further study at pH 3−5 is needed both experimentally and theoretically.

4. Conclusions

Reaction mechanisms of the amide hydrolysis from the protonated, neutral, and deprotonated forms of a model system (*N*-(*o*-carboxybenzoyl)glycine) have been investigated by use of the B3LYP density functional method.

Our calculations reveal that, in contrast with the mechanism for imide formation in which the solvent has little influence on the reaction barrier, in the amide hydrolysis the energy barrier is significantly lower in solution than in the gas phase. In the model reactions, water molecules function both as a catalyst and as a reactant. The reaction mechanism starting from the neutral form of *N*-(*o*-carboxybenzoyl)-L-amino acid, which corresponds to pH 0−3, is concluded to be the most favored. Also, the concerted mechanism **1 → 6 → 7** is more favorable than the direct proton-transfer stepwise mechanism (**1 → 8 → 6 → 7**) and the alternative mechanism of proton transfer through a water molecule (**1a → 8a → 6a → 7a**). This conclusion is in agreement with experimental observations that the optimal pH for amide hydrolysis of *N*-(*o*-carboxybenzoyl)-L-leucine is pH 0−3 where *N*-(*o*-carboxybenzoyl)-L-leucine is predominantly in its neutral form. We suggest that besides the acid-catalyzed mechanism, the addition−elimination mechanism is likely to be an alternative choice for cleaving an amide bond. For the reaction mechanism initiated by protonation at the amidic oxygen (corresponding to hydrogen ion concentration $H_0 < -1$, **1 → 2 → 3 → 4 → 5**), two mechanisms were studied. One is the reaction of the model compound with a single water molecule, and the other is with two water molecules. The calculations show that the reaction of the model compound with two water molecules lowers the transition barrier significantly relative to that with a single water molecule. Finally, the reaction pathway starting from deprotonation at the carboxyl group of the phthalic acid (pH 3−5, **1 → 10 → 11 → 12 → 13**) has not been located and needs to be studied further.

For the hydrogen ion concentration $H_0 < -1$, the solvent raises the transition state, while at pH 0−3, the transition state is lowered. For the transition states **TS3** and **TS5** of the proton transfer (either direct or through a water molecule) at pH 0−3, the solvent does not have much influence on the reaction barrier.

The energy profiles at 0 K show a pattern similar to those at 298.15 K for both phases.

Acknowledgment. We gratefully acknowledge the Natural Sciences and Engineering Research Council of Canada and the Killam Trusts for financial support.

JA021329I